Indonesian Physical Review

Volume 07 Issue 03, September 2024

P-ISSN: 2615-1278, E-ISSN: 2614-7904

Phase and Functional Groups Analysis of ZnO Nanocrystalline Synthesized from Citrus Orange Peel

M. Samsul Ma'arif[1], Fitria Tahta Alfina[2], Devi Ragita Putri Pratiwi[3], Lydia Rohmawati[4*]

[1]Department of Physics, Faculty of Mathematics and Natural Sciences, Universitas Negeri Surabaya, Jl. Ketintang, Surabaya 60231, Indonesia

Corresponding Authors E-mail: lydiarohmawati@unesa.ac.id

Article Info

Article info:

Received: 22-05-2024

Revised: 12-08-2024

Accepted: 15-08-2024

Keywords:

Functional Groups; Phase; Orange Peel; ZnO Nanocrystalline

How To Cite:

M. S. Ma'arif, F. T. Alfina, D. R. P. Pratiwi, and L. Rohmawati, "ZnO Nanocrystalline from Citrus sinensis Orange Peel: Phase and Functional Groups", Indonesian Physical Review, vol. 7, no. 3, p 429-439, 2024.

DOI:

https://doi.org/10.29303/ipr.v7i3.338

Abstract

The high production and market demand for citrus fruits can increase environmental waste. Most people do not use orange peel waste even though this peel contains bioactive compounds and phytochemicals that have the potential to form ZnO using the green synthesis method. This new research offers an environmentally friendly solution to reducing orange peel waste using abundant natural resources for nanotechnology applications. Therefore, this research aims to identify the phase of ZnO material and functional groups from orange peel extract. The extraction method of ZnO from Citrus sinensis orange peel uses green synthesis. The analysis in this research indicates that the sample has the phase of a zincite crystalline and a nanocrystalline size of 12.98 nm. The sample has an absorption peak at a wave number of 4000 – 400 cm^{-1} with functional groups indicating OH, C=C, Zn-OH, and Zn-O stretching vibration.

Introduction

In the industrial sector, interest in organic waste catalytic oxides, including ZnO, has grown recently. Several studies have stated that ZnO quickly reacts with alkaline chemical groups, namely Li, K, and Na. If ZnO is exposed to the skin, it will cause skin irritation [1]. Zinc oxide (ZnO) in nanotechnology has produced various innovative products with broad applications in sectors such as sunscreen, gas sensors, antimicrobial materials, photocatalysts [2], and solar cells [3]. This is because ZnO possesses superior characteristics and properties, including its function as a semiconductor with an energy band gap of 3.37 eV [4] and its nanostructure, which is significant for various reasons, such as low cost, high abundance, and environmentally friendly matrix [5]. In addition, ZnO also has higher chemical resistivity,

good temperature stability [5], and high electron mobility, making it a promising candidate for applications in various fields [6]. ZnO can exist in various phases, such as zincite, wurtzite, and zincblende, formed depending on the synthesis conditions used. In the pursuit of obtaining the desired properties, the synthesis method and composition formula play crucial roles in the manufacturing process of this alloy [7]. Furthermore, the crystals' size, shape, and orientation can be influenced by temperature, reaction time, and the type of precursor used in the synthesis process [1]. Green synthesis ZnO research can use plants, such as aloe vera leaf extract [8], rambutan peel extract [4], Nauclea latifolia fruit extract [9], ginger extract [10], pineapple skin extract [11] and orange peel extract [12]. Orange peel contains several phenolic and flavonoid compounds that can contribute to the metal ion reduction process. According to phytochemical findings, it contains tannins, saponins, phytate oxalate, flavonoids, and limonoids. Limonoids can inhibit the formation of cancer cells, and they have been field-tested on insects [13]. Several ZnO synthesis methods have been developed by several researchers, including sol-gel [14], precipitation [15], thermal decomposition [16], sonochemistry [17], and green synthesis [18].

Research on zinc oxide (ZnO) synthesized using green synthesis methods shows significant differences from conventional synthesis methods often conducted in factories. Traditional methods such as sol-gel, hydrothermal, and co-precipitation typically employ synthetic chemicals like glucose, citric acid, and urea as reductants, operating under extreme conditions such as high temperatures and extreme pH levels [18]. These processes are often environmentally unfriendly due to the use of hazardous chemicals and the generation of waste that is difficult to decompose. On the other hand, green synthesis utilizes natural materials such as plant or microbial extracts, like orange peel extract, as the base material to produce ZnO. This method is more environmentally friendly as it reduces hazardous waste and uses expensive synthetic chemicals [19]. In addition, ZnO produced from green synthesis tends to be more biocompatible and safer for biomedical applications, as it does not contain toxic chemical residues [5]. The study by Dhoan *et al.* illustrated that ZnO synthesized from orange peel extract and zinc nitrate by green synthesis, calcined at 40°C for 60 minutes, showed a weak crystal structure due to the low synthesis temperature [11]. However, increasing the calcination temperature to 900°C increased diffraction peak intensity and crystal size, suggesting that the properties of ZnO can be optimized by proper temperature control in the green synthesis process.

The novelty of this research lies in using orange peel extract as a base material in synthesizing zinc oxide (ZnO) via the green synthesis method, which is a new and environmentally friendly approach. This study combined orange peel extract with 2.5 grams of zinc nitrate and stirred the mixture using ultrasonication for 60 minutes [20], an effective technique for homogenization and particle size control. The applied stepwise calcination process provides better control of the ZnO crystal structure. Characterization using X-ray diffraction (XRD) and Fourier transform infrared spectroscopy (FTIR) provided a complete picture of the structure and chemical composition of the ZnO produced. The resulting ZnO exhibited potent antibacterial activity and high biocompatibility, making it suitable for biomedical applications. This research contributes to developing environmentally friendly ZnO synthesis methods and offers sustainable solutions in various fields of technology and healthcare.

Table 1. Comparison of ZnO Synthesis from Conventional and Green Synthesis Methods

Characteristics	Conventional Method	Green Synthesis
Reductant Materials	Glucose, Nitric Acid, Urea	Orange peel extract
Synthesis Process	Using hazardous chemicals and extreme conditions	Using natural materials, the reaction conditions are more environmentally friendly.
Environment	Not environmentally friendly (hazardous waste)	Environmentally friendly (reduces hazardous waste)
Biocompatibility	Less biocompatible	More biocompatible
Production Costs	Relatively high (use of synthetic chemicals)	Relatively low (using abundant natural raw materials)

Experimental Method

Materials

The materials used to synthesize ZnO are orange peel (*Citrus sinensis*), Zn $(NO_3)_2$ Sigma-Aldrich 99% as a precursor, Zinc, and water distilled as solvent. Some equipment was used for this experiment. For instance, beakers and measuring cups as a medium for pouring material, digital scales as a measurement of the used material, ultrasonication JEKEN PS-A20 to homogenize the solution and accelerate the reaction rate with the help of waves, a stirrer and a magnetic bar for the mixing process, furnace and dry oven for the sample heating process.

Preparation synthesis of Zinc Oxide

The waste orange peel was washed and dried in a dry oven at 90 °C. Afterward, the orange peel was ground using a mortar pestle to obtain orange peel powder. It was stirred by a beaker containing 50 mL of distilled water and 1 gram of orange peel powder with a magnetic stirrer for three hours. The mixture was ultrasonicated at 60°C for 60 minutes, then filtered and obtained the filtrate in the form of *Citrus sinensis* peel extract. Furthermore, ZnO was synthesized by adding 2.5 gr of Zinc Nitrate and 43 mL of orange peel extract. The mixture was ultrasonicated at 60°C for 60 minutes, and the result was heated at 400°C for one hour to get ZnO powder.

Characterization methods

X-ray diffraction (XRD) characterization was done to determine how the primary phase formed in the sample. The samples powder in the form of powder were characterized using an XRD type Xpert MPD system using a Cu radiation source of 35 mA, 40 kV with a wavelength of 1.54 Å and an angle of 2 theta 10° - 80°. The phase that appears at each peak can be identified using QualX software. The Debye-Scherrer formula, which is written as the following equation, can be used to determine the crystalline size of ZnO:

$$D = \frac{K\lambda}{\beta cos\theta} \quad (1)$$

In the following equation, D is the particle size, K is the form factor of the crystal (0.9 - 1), and λ is the X-ray wavelength (0.15 Å). The value of Full Width at Half Maximum (FWHM) is

determined by looking at the half-curve widening of the diffraction peaks in each crystal plane at positions 2θ and is the diffraction angle (degrees).

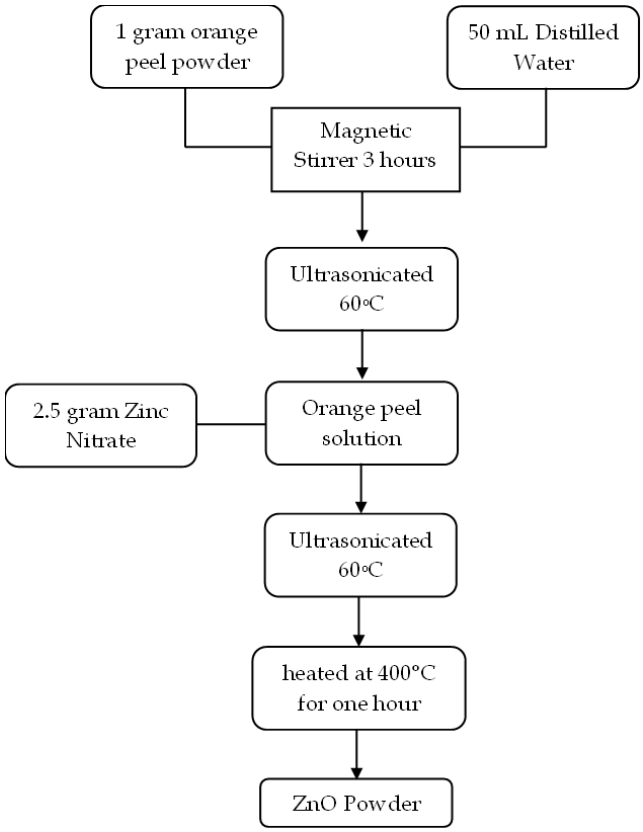

Figure 1. XRD characterization results

At the peak of the ZnO, the spectrum was observed through the Fourier Transform infrared (FT-IR) characterization. The functional groups material and chemical bonds can absorb infrared light rays at specific wavelengths. The energy absorbed by the sample at various frequencies of infrared light was transmitted to the interferometer and converted into an interferogram. The FTIR characterization tool the Shimadzu brand type IR Prestige 21 uses has a wavenumber of 4000 – 400 cm^{-1}. Based on the characterization test, the FTIR spectrum was obtained from the graph showing the relationship between the transmitter mode (%T) and the wavenumber (cm^{-1}). Thus, the result of the wavenumber was compared with the journal reference to investigate the chemical bonds in the sample.

Result and Discussion

Phase analysis

The results of XRD analysis in this research could identify the sample of ZnO phase, crystal structure, and crystallite size. Figure 1 shows the XRD diffraction peaks, which are located at an angle of 2θ, namely 31.72°, 34.42°, 36.21°, 47.51°, 56.59°, 62.86°, 66.45°, 67.83°, 69.14°, 72.42°, 76.92°. They are marked with miller index values (100), (002), (101), (012), (110), (013), (200), (112), (201), (004), and (202). The maximum diffraction peak of ZnO is located at an angle of

36.2° with a crystal orientation (101), following the results of research by [12], which is 36.25° (101) and [19] using *Citrus sinensis* orange peel at an angle of 36.26° (101).

Based on the diffraction angle in Figure 2, ZnO has a hexagonal structure and a zincite phase, according to the JCPSD card with 96-900-4180. In addition, the formed phase shows a 100% Zincite phase without any phase impurities. Equation 1 used the formula of Debye-Scherrer to consider the average crystallite size of ZnO, and the results are shown in Table 2. Each peak has a certain intensity, with a width of FWHM, so the crystallite size value in the sample can be countable. Thus, the average crystallite size in the ZnO sample from the orange peel was 12.98 nm. The crystallite size obtained from this study is less than the result of [12] which used green synthesis to produce ZnO from orange peel at a calcination temperature of 400°C. Crystals of 35-60 nm in size were obtained. The result of crystallite size includes nanocrystalline because it is less than 100 nm [20].

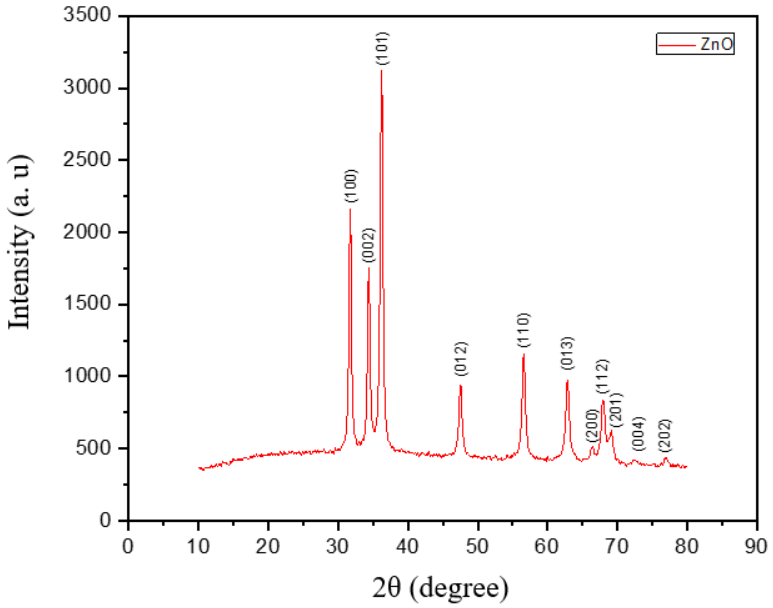

Figure 2. XRD characterization results

There are no additional peaks in this pattern. Rietveld refinement was performed (using Rietica software) on the observed pattern, and various parameter values were calculated. The output of the refinement results in the form of full-width half maxima (FWHM) parameter values are U = 0.000362, V = -0.000237, and W = 0.000050. In addition, the refined plot's Durbin-Watson (D-W) statistical factor is 1.899. The values of profile (Rp), weighted profile (R_{wp}), Bragg (RB), and expected weighted profile factor (R_{exp}) were 3.81, 4.88, 0.58, and 4.41, respectively. The goodness of fit (GoF) is the ratio of the weighted profile and the expected weighted profile factor. The calculated value is 0.1220E+01. The chi-square (X^2) value of the refined plot was 1.220. The chi-square value and the fit indicate that good refinement has been performed. Data analysis shows that the ZnO sample consists of hexagonal unit cells [21]. The synthesized ZnO belongs to the space group P63mc (186). The refined values of the lattice parameters are a=b=3.250497 and c=5.207396 Å. The coordinates of zinc ions in the unit cell are x = 0.33330, y = 0.66670, and z = 0.00000. Similarly, the coordinates of oxygen ions are x =

0.33330, y = 0.66670, and z = 0.38240. The volume of the unit cell is 47.648655, with a density of 15.978. These values are used to build the structural model of ZnO. Zinc and oxygen ions are arranged in layers in the ZnO structure. These layers are placed in a hexagonal shape. The zinc ion is surrounded by four oxygen ions in a tetrahedral configuration, forming a tetrahedron (Figure 3).

Table 2. ZnO crystallite size

No	2θ	FWHM	d-spacing (Å)	Crystallite size (nm)	Average size crystallite size
1	31.7166	0.4886	2.82023	16.90	12.98
2	34.3773	0.5293	2.60496	15.71	
3	36.2056	0.5319	2.48043	15.71	
4	47.5102	0.5848	1.91366	14.84	
5	56.5755	0.6096	1.62635	14.79	
6	62.8439	0.6948	1.47832	13.39	
7	66.5233	1.0488	1.40690	9.060	
8	67.9386	0.9672	1.38164	13.74	
9	69.0392	0.8327	1.35863	11.58	
10	72.4814	0.5853	1.30496	16.83	
11	81.4086	33.0959	1.23945	0.320	

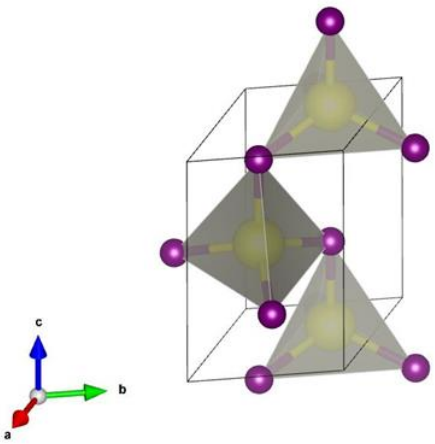

Figure 3. ZnO hexagonal crystal structure using Vesta software [22]

Functional Group Analysis

FTIR (Fourier Transform Infrared Spectroscopy) testing on ZnO samples involves several steps considering the Lambert-Beer law to obtain accurate infrared spectra [23]. The first step is sample preparation, where 0.3 grams of ZnO powder is compressed to form transparent pellets with a diameter of 3 mm and a thickness of 1 mm. These pellets are then placed in a unique holder for FTIR measurements. Next, the pellet is inserted into the sample chamber of the FTIR spectrometer. Infrared light is emitted through the pellets, and the absorbance spectra are measured over a wavelength range of 4000 cm^{-1} to 400 cm^{-1}. The absorbance spectra

obtained indicate the vibrations of the molecules in the ZnO sample. According to the Lambert-Beer law, the absorbance (A) is proportional to the concentration (C) of the absorbing species, the path length (l), and the molar absorptivity coefficient (ϵ) [24]. The peaks in the FTIR spectrum are identified based on their wavelength position and intensity. The chemical structure and functional groups within the ZnO sample can be determined by analyzing the FTIR spectra. The Lambert-Beer equation is [24]:

$$C = \frac{A}{\epsilon\, l} \tag{2}$$

FTIR characterization of the result analysis in the form of peak transmittance data and wave number was used to identify the absorption peak of the synthesized sample concerning the wave number. Figure 3 shows the spectrum of the analysis using FTIR to find functional groups in ZnO produced from orange peel extract by the green synthesis in the wave number range of 4000 – 400 cm^{-1}. Vibration modes in the FTIR spectrum are located at 3372.09, 1440.35, 840.11, 689.43, 466.68, and 447.40 cm^{-1}. The absorption peak of 3372.09 cm^{-1} is identified as stretching function -OH groups [25], which is the absorption of *Citrus sinensis* orange peel extract. [26]. The wave number 3372.09 cm^{-1} is observed to have a broad crest. It depends on the absorption of CO_2 and water molecules on the surface of the synthesized ZnO sample.

The absorption peak of 1440 cm^{-1} has a C=C functional group, which follows what has been reported by [27] at 1411.89 cm^{-1} for ZnO from *Mangifera indica L. anacardiaceae*. 840.11 cm^{-1}, the functional group Zn-OH is identified with weak absorption intensity. Likewise, the absorption peaks of 689.43, 466.68, and 447.40 cm^{-1} have a Zn-O stretching vibration functional group [28], [29], [30] reported that an absorption peak of 600 to 400 cm^{-1} is the characteristic of Zn-O vibration. Thus, the synthesized sample from orange peel has successfully demonstrated the characteristics of ZnO. More details can be seen in Table 3.

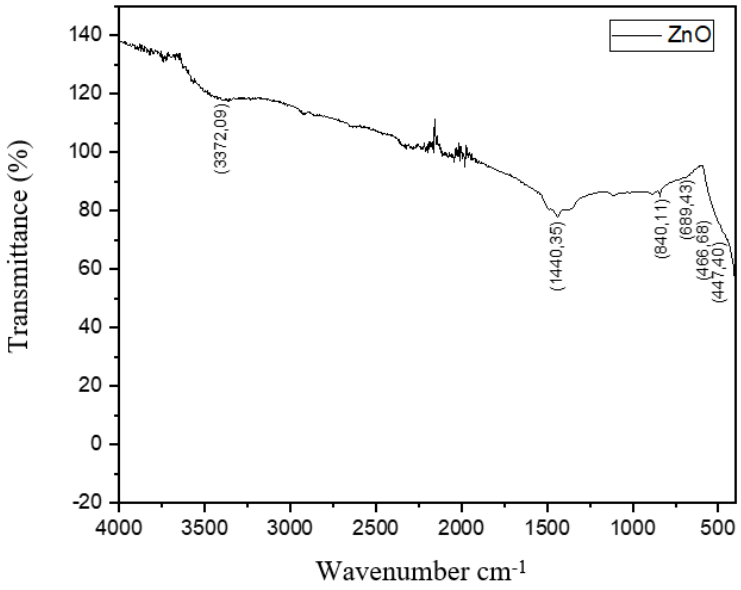

Figure 4. FTIR characterization results

Table 3. Bonding functional groups of ZnO material

No	Wave number		Functional group
	Experiment (cm^{-1})	Reference (cm^{-1})	
1	447.40	400-600 [31]	Zn-O stretching vibration
2	466.68	450 [32]	
3	689.43	617 [29]	Zn-OH
4	840.11	820 [12]	
5	1440.35	1411.89 [27]	C=C
6	3372.09	3380 [33] and 3455 [26]	OH Stretching

Conclusion

The synthesis of ZnO from Citrus sinensis orange peel extract was successfully done using the green synthesis method. XRD characterization results show that the primary phase is zincite (100%), according to the JCPSD card, with several 96-900-4180, and the average size of the nanocrystals was 12.98 nm. The absorption peak is seen through FTIR characterization with a 4000 – 400 cm^{-1} range obtained functional groups of as -OH, C=C, Zn-OH, and Zn-O stretching vibration.

Acknowledgment

Acknowledgments are conveyed to the Institut Teknologi Sepuluh Nopember (ITS) materials and metallurgical laboratory and the material laboratory of the physics department of the mathematics and natural sciences faculty of Universitas Negeri Surabaya for their research facilities.

References

[1] S. Raha and M. Ahmaruzzaman, "ZnO nanostructured materials and their potential applications: progress, challenges, and perspectives," *Nanoscale Adv.*, vol. 4, no. 8, pp. 1868–1925, 2022, doi: 10.1039/d1na00880c.

[2] T. S. Aldeen, H. E. Ahmed Mohamed, and M. Maaza, "ZnO nanoparticles prepared via a green synthesis approach: Physical properties, photocatalytic and antibacterial activity," *J. Phys. Chem. Solids*, vol. 160, no. August 2021, p. 110313, 2022, doi: 10.1016/j.jpcs.2021.110313.

[3] M. Manabeng, B. S. Mwankemwa, R. O. Ocaya, T. E. Motaung, and T. D. Malevu, "A Review of the Impact of Zinc Oxide Nanostructure Morphology on Perovskite Solar Cell Performance," *Processes*, vol. 10, no. 9, pp. 1–19, 2022, doi: 10.3390/pr10091803.

[4] C. Hernández-Hernández *et al.*, "Rambutan(Nephelium lappaceum L.):Nutritional and functional properties," *Trends Food Sci. Technol.*, vol. 85, no. September 2018, pp. 201–210, 2019, doi: 10.1016/j.tifs.2019.01.018.

[5] A. Sharif, M. Mustaqeem, T. A. Saleh, A. ur Rehman, M. Ahmad, and M. F. Warsi, "Synthesis, structural and dielectric properties of Mg/Zn ferrites -PVA nanocomposites," *Mater. Sci. Eng. B*, vol. 280, no. April, p. 115689, 2022, doi: 10.1016/j.mseb.2022.115689.

[6] L. Li, X. Guo, X. Lu, J. Ren, and P. La, "Electronic and photocatalytic properties of ZnO/GaTe heterostructure from first principles calculations," *Mater. Sci. Semicond.*

Process., vol. 154, no. October 2022, p. 107189, 2023, doi: 10.1016/j.mssp.2022.107189.

[7] I. Ali *et al.*, "Zn/Ba nanoparticles doping effect on surface interface, Morphology, and dielectric elucidation of spinel ferrites," *Surfaces and Interfaces*, vol. 38, no. March, p. 102862, 2023, doi: 10.1016/j.surfin.2023.102862.

[8] C. Wu, T. Zhang, B. Ji, Y. Chou, and X. Du, "Green Synthesis of Zinc Oxide Nanoparticles Using Aloe Vera Leaves Extract and Evaluation of ALE-ZnO/Regenerated Cellulose Films Antibacterial, Antioxidant Properties," *J. Nanomater.*, vol. 2023, no. 0123456789, pp. 1–14, 2023, doi: 10.1007/s10570-024-05914-9.

[9] S. M. Abegunde, E. F. Olasehinde, and M. A. Adebayo, "Green synthesis of ZnO nanoparticles using Nauclea latifolia fruit extract for adsorption of Congo red," *Hybrid Adv.*, vol. 5, no. February, p. 100164, 2024, doi: 10.1016/j.hybadv.2024.100164.

[10] M. Aliannezhadi, S. Z. Mirsanaee, M. Jamali, and F. Shariatmadar Tehrani, "The physical properties and photocatalytic activities of green synthesized ZnO nanostructures using different ginger extract concentrations," *Sci. Rep.*, vol. 14, no. 1, pp. 1–13, 2024, doi: 10.1038/s41598-024-52455-z.

[11] R. S. P. Dewi and L. Rohmawati, "ANALYSIS OF CRYSTALLINE PHASE AND FUNCTIONAL GROUPS OF ZnO FROM PINEAPPLE PEEL EXTRACT," *Indones. Phys. Rev.*, vol. 5, no. 3, pp. 148–156, Jul. 2022, doi: 10.29303/ipr.v5i3.160.

[12] T. U. Doan Thi, T. T. Nguyen, Y. D. Thi, K. H. Ta Thi, B. T. Phan, and K. N. Pham, "Green synthesis of ZnO nanoparticles using orange fruit peel extract for antibacterial activities," *RSC Adv.*, vol. 10, no. 40, pp. 23899–23907, 2020, doi: 10.1039/d0ra04926c.

[13] Godfred Yaw Boanyah and Prince Yaw Boakye, "Natural repellents a topic not to be neglected in a quest for new effective mosquito repellent: A review on Azardirachta indica (neem) and Citrus sinensis (sweet orange)," *GSC Adv. Res. Rev.*, vol. 13, no. 2, pp. 150–157, 2022, doi: 10.30574/gscarr.2022.13.2.0331.

[14] M. Mustaqeem *et al.*, "Synthesis of CuFe2–xErxO4 nanoparticles and their magnetic, structural and dielectric properties," *Phys. B Condens. Matter*, vol. 588, no. February, 2020, doi: 10.1016/j.physb.2020.412176.

[15] H. Hamrayev and K. Shameli, "Biopolymer-Based Green Synthesis of Zinc Oxide (ZnO) Nanoparticles," *IOP Conf. Ser. Mater. Sci. Eng.*, vol. 1051, no. 1, p. 012088, 2021, doi: 10.1088/1757-899x/1051/1/012088.

[16] D. B. Bharti and A. V. Bharati, "Synthesis of ZnO nanoparticles using a hydrothermal method and a study its optical activity," *Luminescence*, vol. 32, no. 3, pp. 317–320, 2017, doi: 10.1002/bio.3180.

[17] A. Maddu, Zetria Zikri, and I. Irzaman, "Structure and Morphology of ZnO Nanoparticles Prepared by Sonochemical Method," *TIME Phys.*, vol. 1, no. 2, pp. 51–58, 2023, doi: 10.11594/timeinphys.2023.v1i2p51-58.

[18] M. A. Albo Hay Allah and H. A. Alshamsi, "Green synthesis of ZnO NPs using Pontederia crassipes leaf extract: characterization, their adsorption behavior and anti-cancer property," *Biomass Convers. Biorefinery*, pp. 10487–10500, 2022, doi: 10.1007/s13399-022-03091-y.

[19] H. Çolak and E. Karaköse, "Green synthesis and characterization of nanostructured ZnO thin films using Citrus aurantifolia (lemon) peel extract by spin-coating method," *J. Alloys Compd.*, vol. 690, pp. 658–662, 2017, doi: 10.1016/j.jallcom.2016.08.090.

[20] T. Tangcharoen, "Influence of non-magnetic ions doping on structural, morphological, optical, and magnetic properties of nanocrystalline zinc oxide powders," *Phys. B Condens. Matter*, vol. 663, no. May, 2023, doi: 10.1016/j.physb.2023.415010.

[21] S. Jamil, T. Tariq, S. R. Khan, M. A. Ehsan, A. Rehman, and M. R. S. A. Janjua, "Structural Characterization, Synthesis and Application of Zincite Nanoparticles as Fuel Additive," *J. Clust. Sci.*, vol. 33, no. 3, pp. 1165–1176, 2022, doi: 10.1007/s10876-021-02047-y.

[22] K. Momma and F. Izumi, "VESTA: Visualization for Electronic and Structural Analysis." National Museum of Nature and Science, 4-1-1 Amakubo, Tsukuba, Ibaraki 305-0005, Japan, 2020. [Online]. Available: https://jp-minerals.org/vesta/en/

[23] A. Villegas-Fuentes, H. E. Garrafa-Gálvez, R. V. Quevedo-Robles, M. Luque-Morales, A. R. Vilchis-Nestor, and P. A. Luque, "Synthesis of semiconductor ZnO nanoparticles using Citrus microcarpa extract and the influence of concentration on their optical properties," *J. Mol. Struct.*, vol. 1281, 2023, doi: 10.1016/j.molstruc.2023.135067.

[24] R. Delgado, "Misuse of Beer-Lambert Law and other calibration curves," *R. Soc. Open Sci.*, vol. 9, no. 2, 2022, doi: 10.1098/rsos.211103.

[25] W. Hassan, M. Mustaqeem, U. Farooq, S. Noureen, D. H. Gregory, and T. A. Saleh, "Pengaruh modifikasi biomassa Haloxylon recurvum terhadap penyerapan zat warna asam dari media berair," pp. 4813–4827, 2024.

[26] Y. Gao, D. Xu, D. Ren, K. Zeng, and X. Wu, "Green synthesis of zinc oxide nanoparticles using Citrus sinensis peel extract and application to strawberry preservation: A comparison study," *Lwt*, vol. 126, no. December 2019, p. 109297, 2020, doi: 10.1016/j.lwt.2020.109297.

[27] S. U. Geetha and S. Thilakavathy, "FTIR and XRD of Zinc Oxide Nano Particle from Mangifera indica L. anacardiaceae," *J. Pharm. Res. Int.*, vol. 33, pp. 176–181, 2021, doi: 10.9734/jpri/2021/v33i47a33001.

[28] T. Bhuyan, K. Mishra, M. Khanuja, R. Prasad, and A. Varma, "Biosynthesis of zinc oxide nanoparticles from Azadirachta indica for antibacterial and photocatalytic applications," *Mater. Sci. Semicond. Process.*, vol. 32, pp. 55–61, 2015, doi: 10.1016/j.mssp.2014.12.053.

[29] D. Zewde and B. Geremew, "Biosynthesis of ZnO nanoparticles using Hagenia abyssinica leaf extracts; their photocatalytic and antibacterial activities," *Environ. Pollut. Bioavailab.*, vol. 34, no. 1, pp. 224–235, 2022, doi: 10.1080/26395940.2022.2081261.

[30] P. C. Nagajyothi, S. J. Cha, I. J. Yang, T. V. M. Sreekanth, K. J. Kim, and H. M. Shin, "Antioxidant and anti-inflammatory activities of zinc oxide nanoparticles synthesized using Polygala tenuifolia root extract," *J. Photochem. Photobiol. B Biol.*, vol. 146, pp. 10–17, 2015, doi: 10.1016/j.jphotobiol.2015.02.008.

[31] B. Darbasizadeh *et al.*, "Crosslinked-polyvinyl alcohol-carboxymethyl cellulose/ZnO nanocomposite fibrous mats containing erythromycin (PVA-CMC/ZnO-EM): Fabrication, characterization and in-vitro release and anti-bacterial properties," *Int. J. Biol. Macromol.*, vol. 141, pp. 1137–1146, 2019, doi: 10.1016/j.ijbiomac.2019.09.060.

[32] R. Ahmed *et al.*, "Novel electrospun chitosan/polyvinyl alcohol/zinc oxide nanofibrous mats with antibacterial and antioxidant properties for diabetic wound healing," *Int. J. Biol. Macromol.*, vol. 120, pp. 385–393, 2018, doi: 10.1016/j.ijbiomac.2018.08.057.

[33] N. A. Mirgane, V. S. Shivankar, S. B. Kotwal, G. C. Wadhawa, and M. C. Sonawale, "Waste pericarp of ananas comosus in green synthesis zinc oxide nanoparticles and their application in waste water treatment," *Mater. Today Proc.*, vol. 37, no. Part 2, pp. 886–889, 2020, doi: 10.1016/j.matpr.2020.06.045.